Self-Selective Silver Modification of SiO Anodes: A Conductivity-Boosting Strategy for High-Performance Lithium-Ion Batteries

Asif Raza,[a,b†], Panjin Noh[a,†], Jaehyuk Yang[a,†,a,d], Mukarram Ali[a], Minjoon Park[d,], Hae-Young Choi[a*] Sang-Min Lee,[c*]*

[a] Next Generation Battery Research Center, Korea Electrotechnology Research Institute, 12, Bulmosan–ro 10 beon–gil, Seongsan–gu, Changwon–si, Gyeongsangnam–do 51543, Republic of Korea

[b] Department of Chemistry, University of Ulsan, TechnoSanup-ro 55-gil 12, Nam-gu, Ulsan 44776, Rep. of Korea

[c] Graduate Institute of Ferrous & Energy Materials Technology (GIFT), Pohang University of Science and Technology, 77 Cheongam-Ro, Nam-Gu, Pohang, Gyeongbuk, 37673, Republic of Korea

[d] Department of Nanoenergy Engineering, Department of Nano Fusion Technology, Research Center of Energy Convergence Technology Pusan National University, 50, Busan daehak-ro 63 beon-gil 2, Geumjeong-gu, Busan 46241, Republic of Korea

Supplementary Information

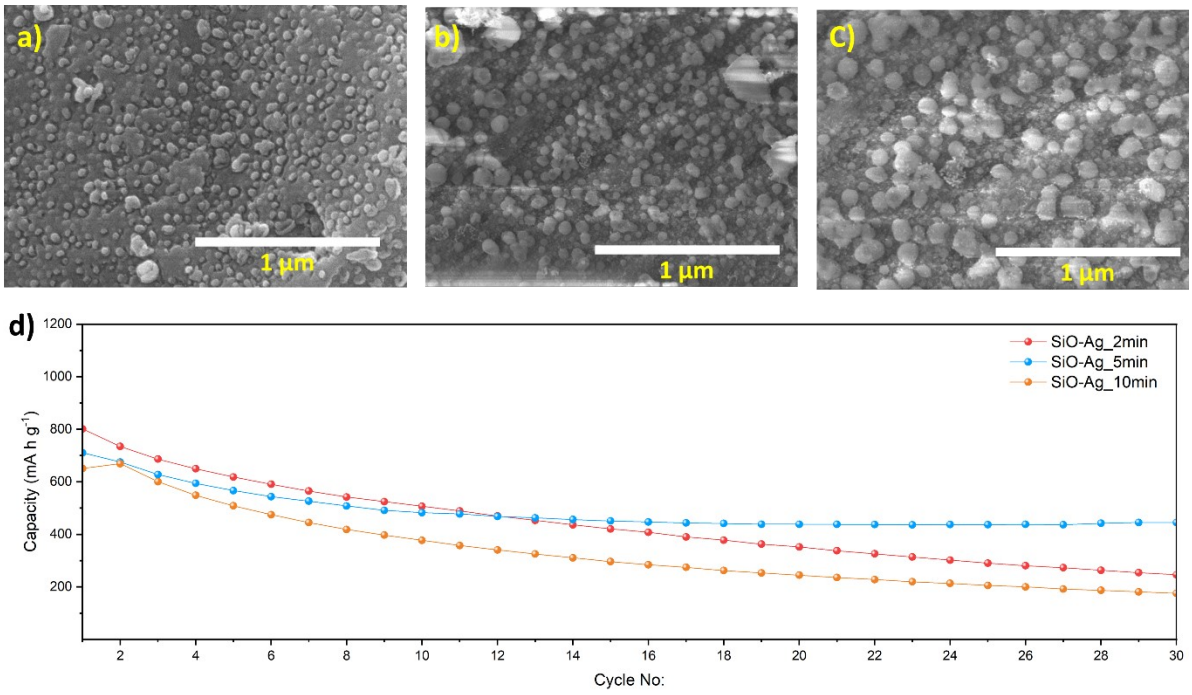

Figure S1: SEM images of Ag-doped SiO at different deposition times: (a) 5 min, (b) 10 min, and (c) 15 min. (d) cycle data for optimal sample at 1.0C

SEM images for SiO-Ag electrodes with different silver deposition time, (a) 2min, (b) 5min and (c) 10min. The figure (d) demonstrates the cycling performance of SiO-Ag electrodes with different silver deposition times, namely 2, 5, and 10 min. As seen in the graph, the capacity of the SiO-Ag electrodes decreases with cycling, but the electrode deposited for 5 minutes shows the highest capacity retention compared to other samples, suggesting an optimal Ag doping level for enhanced electrochemical stability. The sample with a 5-minute deposition time of silver was chosen for this study and noted as SiO-Ag. Ag mainly functions as a conductive component rather than an active Li-storage material. Therefore, its content requires careful balance: too little Ag may not form an effective conductive network to enhance charge transport, whereas excessive Ag can reduce the fraction of electrochemically active SiO and potentially increase surface reactivity with the electrolyte. In this study, the Ag content (~16 wt%), obtained under optimized deposition

conditions, provides a suitable balance between improved electronic conductivity and maintaining sufficient active material for Li storage.

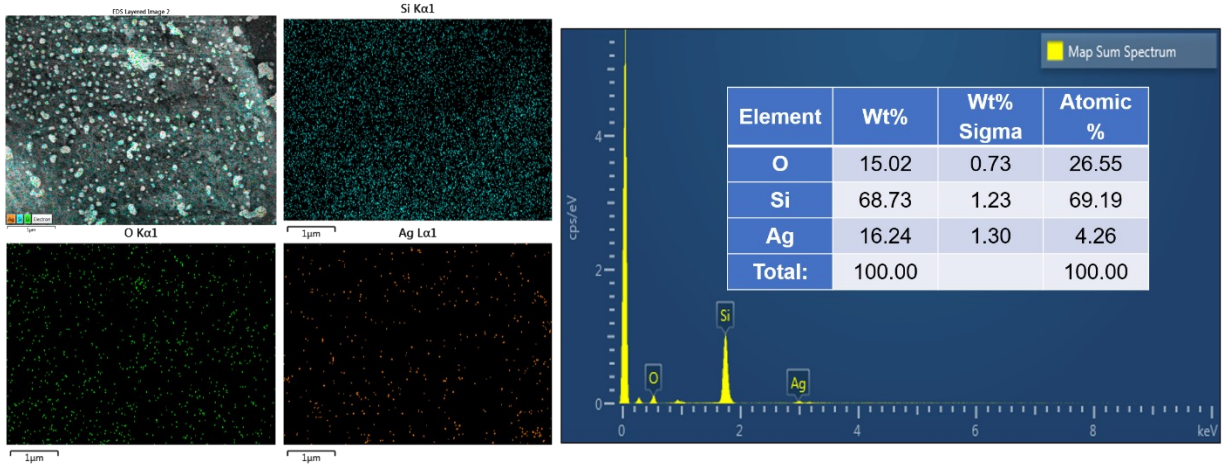

Figure S2: SEM EDX images for SiO-Ag

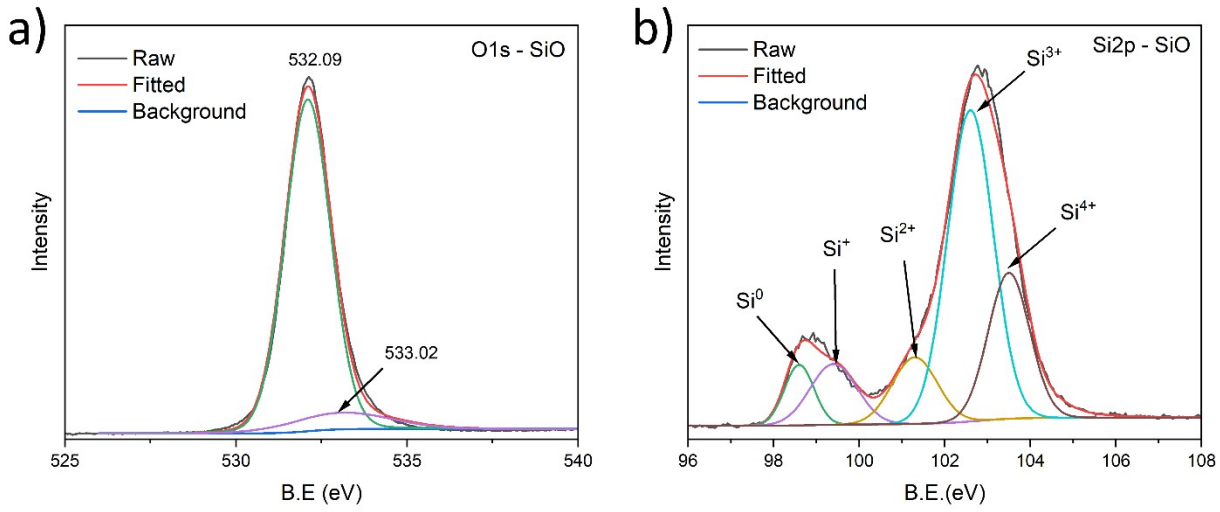

Figure S3: XPS spectra of (a) O1s and (b) Si2p for SiO.

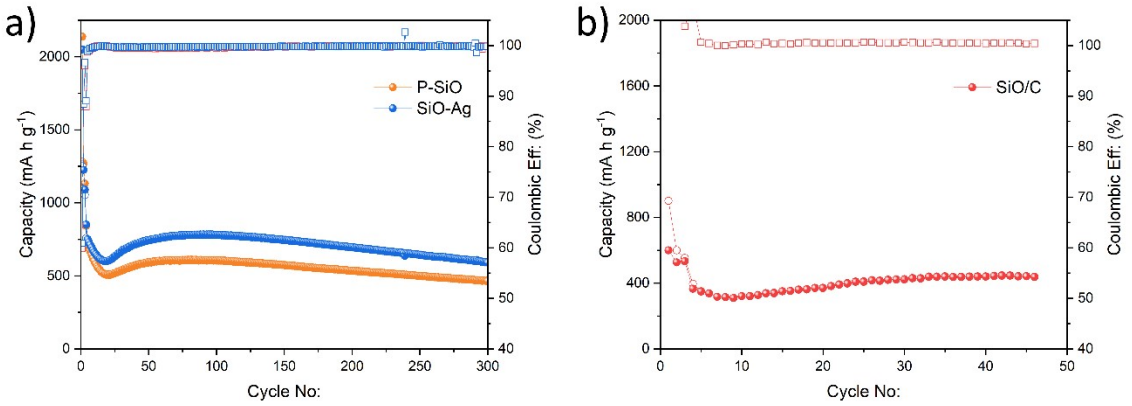

Figure S4: Electrochemical cyclic data for the comparison of (a) SiO-Ag and P-SiO (Ag etched), (b) SiO/C at 0.5C.

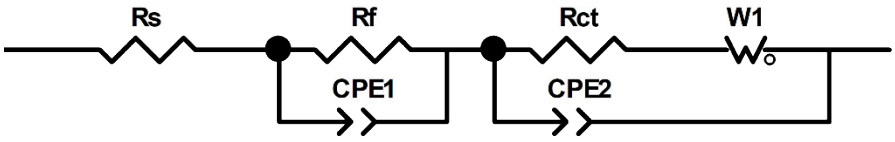

SiO	
R1+R2/Q2+(R3+W3)/Q3	
R1 = 20.15 Ohm	
R2 = 8.091e27 Ohm	
Q2 = 0.282 6e-3 F.s^(a - 1)	
a2 = 0.850 7	
R3 = 1 053 Ohm	
s3 = 1.07 Ohm.s^-1/2	
Q3 = 16.25e-6 F.s^(a - 1)	
a3 = 0.681 5	

SiO-Ag	
R1+R2/Q2+(R3+W3)/Q3	
R1 = 1.52 Ohm	
R2 = 70.35 Ohm	
Q2 = 24.77e-6 F.s^(a - 1)	
a2 = 0.769 5	
R3 = 20 102 Ohm	
s3 = 0.023 07 Ohm.s^-1/2	
Q3 = 0.234 7e-3 F.s^(a - 1)	
a3 = 0.797 6	

$$D_{Li^+} = \frac{R^2T^2}{2n^4F^4A^2C_s^2\sigma^2}$$

A = 1.539 cm² (electrode surface area)

C_s = 0.0113 mol/cm³ (Li^+ concentration in the electrode)

Figure S5: Equivalence circuit and fitting data for SiO and SiO-Ag composite.

Table S1: The Comparative summary of electrochemical performance for reported carbon-coated and modified SiO-based anodes for LIBs. Values are shown for qualitative comparison, as testing conditions vary across studies.

Material / Strategy	**Synthesis Method**	**Initial Capacity (mAh g^{-1})**	**ICE (%)**	**Capacity Retention**	**Reff:**
Si/Ag@SiO_x	self-selective electroless deposition + wet oxidation in a sealed Teflon-lined autoclave	2798 at 0.42 A g^{-1}	Not reported	1453 after 100 cycles at 8.4 A g^{-1}	[1]
phosphorus-modified SiO/C	Ball Milling + Sintering	846 at 0.1 A g^{-1}	77.0	545 after 300 cycles at 8.4 0.5 A g^{-1}	[2]
SiO/graphite@C	fluidization thermal chemical vapor deposition	852.6 at 100 mA g^{-1}	86.0	799 after 100 cycles (93.7%) at 200 mA g^{-1}	[3]
carbon-coated SiO_x/Ag	self-selective electroless deposition + Ball Milling	1918 at 0.042 A g^{-1}	71.5	1102 after 150 cycles at ~1 A g^{-1}	[4]
SiO@C/TiO_2	ball milling and sol-gel method,	1590 at 0.1 A g^{-1}	97	844 after 220 cycles at 0.2 A g^{-1}	[5]
TiO_{2-x}@SiO/C	Ag-assisted chemical etching process followed by a hydrolysis approach	1098 at 0.2 A g^{-1}	Not reported	423 after 300 cycles at 2.0 A g^{-1}	[6]
PSi@SiO_x/Nano-Ag composite	Oxidation and chemical reduction method	3033 at 500 mA g^{-1}	86.9	1409 after 500 cycles at 200 mA g^{-1}	[7]
MOF-derived SiO@C	ZIF-8 template + pyrolysis	641 at 100 mA g^{-1}	38.1	46.8% after 500 cycles t 100 mA g^{-1}	[8]
SiO@C-L	Layer-by-layer strategy	Not reported	51.18	699 after 700 cycles (85%) @ 1 Ag^{-1}	[9]

SiO–1D–C/a–C	fluidized bed chemical vapor deposition	1202 at 0.1 A g^{-1}	70.2	1012 after 120 cycles at 0.5 A g^{-1}	[10]
SiO@C-Al_2O_3	Ball-milling + pyrolysis reaction	471 at 100 mA g^{-1}	65.9	~453 after 300 cycles at 100 mA g^{-1}	[11]
Biomass-derived SNTs@C	Biomass pyrolysis with Si source	661 at 100 mA g^{-1}	Not reported	549 after 800 cycles @ 1000 mA g^{-1}	[12]
Bamboo-like SiO_x/C nanotubes	St¨ober method and polymer coating	921 @ 100 mA g^{-1}	64.6	702 and 511 at 0.1 and 0.5 A g^{-1}	[13]
Si/Ag@C	Recycling refinery waste + carbonization	1521 at 0.2 A g^{-1}	82.8	706 after 300 cycles at 1 A g^{-1}	[14]
SiO-Ag	Electroless deposition	2050.5 at 0.15 A g^{-1}	60.9	386 after 1000 cycles @ 1C (75%)	This work

Table S2: Comparison of Warburg coefficient (σ) and lithium-ion diffusion coefficient (D_{Li}^{+}) for SiO and SiO-Ag samples.

Sample	**σ (Ω·$s^{-1/2}$)**	**D_{Li}^{+} (cm^2/s)**
SiO	0.2149	2.53×10^{-9}
SiO-Ag	0.02307	2.19×10^{-7}

1 G. Xu, C. Jin, Y. Lan, L. Liu, K. Kong, X. Yang, Z. Yue, X. Li, F. Sun and H. Huang, *Mater. Lett.*, 2018, **233**, 228–232.

2 F. Song, X. Yang, S. Zhang, L.-L. Zhang and Z. Wen, *Ceram. Int.*, 2018, **44**, 18509–18515.

3 M. Xia, Y. Li, Z. Zhou, Y. Wu, N. Zhou, H. Zhang and X. Xiong, *Ceram. Int.*, 2019, **45**, 1950–1959.

4 P. Ouyang, C. Jin, G. Xu, X. Yang, K. Kong, B. Liu, J. Dan, J. Chen, Z. Yue and X. Li, *Ceram. Int.*, 2021, **47**, 1086–1094.

5 L. Liu, X. Li, G. He, G. Zhang, G. Su and C. Fang, *J. Alloys Compd.*, 2020, **836**, 155407.

6 Y. Xu, Y. Li, Y. Qian, S. Sun, N. Lin and Y. Qian, *Inorg. Chem. Front.*, 2023, **10**, 1176–1186.

7 F. Xi, Z. Zhang, Y. Hu, S. Li, W. Ma, X. Chen, X. Wan, C. Chong, B. Luo and L. Wang, *J. Hazard. Mater.*, 2021, **414**, 125480.

8 L. Feng, X. Han, X. Su, B. Pang, Y. Luo, F. Hu, M. Zhou, K. Tao and Y. Xia, *J. Alloys Compd.*, 2018, **765**, 512–519.

9 J. Han, G. Chen, T. Yan, H. Liu, L. Shi, Z. An, J. Zhang and D. Zhang, *Chem. Eng. J.*, 2018, **347**, 273–279.

10 H. Shi, H. Zhang, X. Li, Y. Du, G. Hou, M. Xiang, P. Lv and Q. Zhu, *Carbon N. Y.*, 2020, **168**, 113–124.

11 K. Kim, H. Choi and J.-H. Kim, *Appl. Surf. Sci.*, 2017, **416**, 527–535.

12 D. Sui, M. Yao, L. Si, K. Yan, J. Shi, J. Wang, C. C. Xu and Y. Zhang, *Carbon N. Y.*, 2023, **205**, 510–518.

13 Z. Wang, L. Kong, Z. Guo, X. Zhang, X. Wang and X. Zhang, *Chem. Eng. J.*, 2022, **428**, 131060.

14 Y. Li, G. Chen, W. Liu, L. Huang and X. Luo, *Waste Manag.*, 2023, **156**, 22–32.